The ISME Journal (2013) 7, 800–816
© 2013 International Society for Microbial Ecology All rights reserved 1751-7362/13
www.nature.com/ismej

ORIGINAL ARTICLE

Biostimulation induces syntrophic interactions that impact C, S and N cycling in a sediment microbial community

Kim M Handley[1,4], Nathan C VerBerkmoes[2,5], Carl I Steefel[3], Kenneth H Williams[3], Itai Sharon[1], Christopher S Miller[1], Kyle R Frischkorn[1], Karuna Chourey[2], Brian C Thomas[1], Manesh B Shah[2], Philip E Long[3], Robert L Hettich[2] and Jillian F Banfield[1,3]
[1]*Department of Earth and Planetary Science, University of California, Berkeley, CA, USA;* [2]*Chemical Sciences and Biosciences Divisions, Oak Ridge National Laboratory (ORNL), Oak Ridge, TN, USA and* [3]*Earth Science Division, Lawrence Berkeley National Laboratory (LBNL), Berkeley, CA, USA*

Stimulation of subsurface microorganisms to induce reductive immobilization of metals is a promising approach for bioremediation, yet the overall microbial community response is typically poorly understood. Here we used proteogenomics to test the hypothesis that excess input of acetate activates complex community functioning and syntrophic interactions among autotrophs and heterotrophs. A flow-through sediment column was incubated in a groundwater well of an acetate-amended aquifer and recovered during microbial sulfate reduction. *De novo* reconstruction of community sequences yielded near-complete genomes of *Desulfobacter* (*Deltaproteobacteria*), *Sulfurovum*- and *Sulfurimonas*-like *Epsilonproteobacteria* and *Bacteroidetes*. Partial genomes were obtained for *Clostridiales* (*Firmicutes*) and *Desulfuromonadales*-like *Deltaproteobacteria*. The majority of proteins identified by mass spectrometry corresponded to *Desulfobacter*-like species, and demonstrate the role of this organism in sulfate reduction (Dsr and APS), nitrogen fixation and acetate oxidation to CO_2 during amendment. Results indicate less abundant *Desulfuromonadales*, and possibly *Bacteroidetes*, also actively contributed to CO_2 production via the tricarboxylic acid (TCA) cycle. Proteomic data indicate that sulfide was partially re-oxidized by *Epsilonproteobacteria* through nitrate-dependent sulfide oxidation (using Nap, Nir, Nos, SQR and Sox), with CO_2 fixed using the reverse TCA cycle. We infer that high acetate concentrations, aimed at stimulating anaerobic heterotrophy, led to the co-enrichment of, and carbon fixation in *Epsilonproteobacteria*. Results give an insight into ecosystem behavior following addition of simple organic carbon to the subsurface, and demonstrate a range of biological processes and community interactions were stimulated.

The ISME Journal (2013) **7,** 800–816; doi:10.1038/ismej.2012.148; published online 29 November 2012
Subject Category: Integrated genomics and post-genomics approaches in microbial ecology
Keywords: autotroph; metagenomics; proteomics; sediment; subsurface; syntrophy

Introduction

The role of microorganisms in organic carbon cycling is of considerable interest, as these activities can impact carbon turnover rates and sequestration (Karl *et al.*, 2012) and influence the fate of contaminants, such as petroleum (Hazen *et al.*, 2010), uranium (Anderson *et al.*, 2003) or arsenic (Islam *et al.*, 2004). Sediments host a substantial proportion of the environmental bacterial and archaeal biomass, with an estimated 6–40% of the prokaryotic biomass inhabiting the terrestrial subsurface, and an estimated total carbon content rivaling that of the global plant biomass (Whitman *et al.*, 1998). Most endogenous organic matter in terrestrial sediment is considered to be relatively refractory, consisting largely of polymers, such as lignin and cellulose, and plant-derived (or even petroleum-based) hydrocarbons (Hartog *et al.*, 2004; Rowland *et al.*, 2006). However, some fractions of complex organic matter can be degraded by fermentative or respiratory microorganisms (Benner *et al.*, 1984; Leschine, 1995; Widdel and Rabus, 2001).

In anaerobic environments, such as the terrestrial subsurface, acetate is an important product of central carbohydrate degradation pathways,

Correspondence: JF Banfield, Department of Earth and Planetary Science, University of California, 307 McCone Hall, Berkeley, CA 94720-4767, USA.
E-mail: jbanfield@berkeley.edu
[4]Current address: Computation Institute, University of Chicago, Searle Chemistry Laboratory, 5735 South Ellis Avenue, Chicago, IL 60637, USA; Computing, Environment and Life Sciences, Argonne National Laboratory, 9700 South Cass Avenue, Argonne, IL 60439, USA.
[5]Current address: New England Biolabs, Ipswich, MA 01938, USA.
Received 11 June 2012; revised 28 September 2012; accepted 8 October 2012; published online 29 November 2012

following the oxidation of pyruvate. It is also a common product of respiration or fermentation of other organic acids and alcohols by anaerobic microorganisms, including sulfate-reducing bacteria (SRB) that incompletely oxidize organic matter (Gibson, 1990). Characteristic pathways identified through which acetate oxidation to CO_2 proceeds are the TCA cycle and the acetyl-CoA pathway (Thauer *et al.*, 1989). Both pathways are reversible and can be used by autotrophic bacteria to catalyze the reduction of CO_2 to back to acetyl-CoA (Fuchs, 1986). Acetate can be used in methanogenesis, and numerous bacteria can couple acetate oxidation to the reduction of inorganic compounds, such as Fe(III), U(VI), nitrate, S^0 and sulfate (Thauer *et al.*, 1989; Lovley *et al.*, 2004). As a biologically relevant and non-fermentable organic compound, acetate is an attractive substrate to use in studying biogeochemical cycling linked to anaerobic respiration and bioremediation (Anderson *et al.*, 2003).

While relatively few organisms proliferate when stimulating sediment microbial communities with acetate (Holmes *et al.*, 2002), the enriched organisms constitute a community that is nonetheless intricate (Handley *et al.*, 2012). Community processes can be expected to include syntrophic interactions, biomass recycling, and the precipitation of diverse and in some cases, cryptic biogeochemical cycles. Unraveling the individual roles of community members, and their metabolic pathways is non-trivial.

Here, we used genomics-informed proteomic information (proteogenomics, Ram *et al.*, 2005) to resolve organism-specific activity and detect metabolic pathways utilized in an acetate-amended, sediment-hosted subsurface microbial community, *a priori*. The study provides a snapshot of community-wide functioning and interactions in an aquifer setting during acetate-induced uranium bioremediation under predominantly sulfate-reducing conditions, and builds on previous studies considering the role of bacteria, in particular *Geobacter*, in Fe(III) and U(VI) reduction within the aquifer (for example, Anderson *et al.*, 2003; Holmes *et al.*, 2009; Wilkins *et al.*, 2009; Williams *et al.*, 2011). Our proteogenomic data demonstrate the activity of bacteria linked to metal reduction, in addition to microbial utilization of the carbon, nitrogen and sulfur, and the indirect stimulation of autotrophic (or mixotrophic) bacteria in response to CO_2 and sulfide generated through acetate-dependent sulfate reduction. Biogeochemical reaction modeling was also used to evaluate denitrification pathways.

Materials and methods

Experiment setup and sampling

Un-amended and acetate-amended sediments were sampled from an alluvial freshwater aquifer underlying the Department of Energy's Integrated Field Research Challenge (IFRC) site at Rifle, CO, USA. In order to stimulate aquifer sediment with acetate *in situ*, and access sediment from the subsurface post-stimulation, we incubated sediment in a flow-through column in an existing groundwater well (P104; see well gallery in Williams *et al.*, 2011). Un-amended sediment was first excavated from the aquifer using a backhoe, and sieved (to remove rocks) to a final particle size of <2 mm. This material was packed into a clear custom built PVC cylindrical column (5.1 cm wide $\times$ 10.2 cm long) and incubated $\sim$5 m below ground surface within the well (Supplementary Figure S1). The column equilibrated with subsurface conditions for 15 days before amendment, which have previously been shown to be anoxic with <16 μM of dissolved oxygen (Williams *et al.*, 2011). Acetate (electron donor and carbon source) and bromide (conservative tracer) were injected into wells $\sim$0.5 m upgradient of well P104, obtaining final concentrations of $\sim$15 and $\sim$1.3 mM, respectively (method in Williams *et al.*, 2011). Amended groundwater was pumped up through the column for 24 days, as described previously (Handley *et al.* 2012), during which this region of the aquifer was subject to its third consecutive summer of acetate amendment. Sediment from the entire column was homogenized and then flash frozen upon collection. Comparative analyses with a replicate column and other aquifer samples are described elsewhere (Handley *et al.,* 2012).

Geochemistry analyses

Groundwater samples were filtered using 0.25 μm PTFE filters for geochemical analyses. Acetate, bromide, sulfate, chloride, uranium, Fe(II) and sulfide were measured, as described previously (Williams *et al.* 2011).

DNA extraction

Genomic DNA was extracted from 5 g of un-amended sediment and 300 g of acetate-amended sediment (5–10 g per tube) using PowerMax Soil DNA Isolation Kits (MoBio Laboratories, Inc., Carlsbad, CA, USA) with the following modification to the manufacturer's instructions. Sediment was vortexed at maximum speed for an additional 2 min in SDS, and then incubated for 30 min at 60 °C instead of bead beating. Acetate-amended sediment extraction replicates were pooled in order to obtain $\sim$8 μg of DNA for downstream analysis. All eluted DNA was concentrated, as described by Handley *et al.* (2012).

16S rRNA gene clone libraries

DNA was amplified using the general bacterial 16S rRNA gene primers 27f and 1492r (Lane, 1991), and a temperature gradient to minimize PCR bias, which comprised 11 PCR reactions at 11 different annealing temperatures. The PCR protocol was: 1 min at

94 °C; 25 cycles of 1 min at 94 °C, 30 s at 48–58 °C (11 temperature gradient) and 1 min at 72 °C; and 7 min at 72 °C. Amplicons were pooled, and precipitated as above. Clone libraries were constructed using the TOPO TA Cloning Kit (Invitrogen, Carlsbad, CA, USA) with electrocompetent cells. 16S rRNA genes from transformed colonies were PCR amplified using the protocol: 10 min at 95 °C; 25 cycles of 30 s at 95 °C, 30 s at 53 °C and 1.5 min at 72 °C; and 7 min at 72 °C. Inserts were screened for correct size (~1400 bp) by gel electrophoresis, and sequenced using capillary electrophoresis (Applied Biosystems 3730xl DNA Analyzer, Foster City, CA, USA), with M13f (−21) and M13r (−24) primers (Invitrogen). Sequences were trimmed to remove Phred quality scores ⩽20, and forward and reverse strands were merged into near full-length sequences using Phrap (http://www.phrap.org/phredphrapconsed.html). USEARCH (Edgar, 2010) was used to check for chimeras—after which 98 sequences were retained for each sample (un-amended and acetate-amended)—and to cluster sequences into OTUs 97% similar. A representative from each OTU was BLASTed (Altschul *et al.*, 1990) to a non-redundant version of SILVA SSURef102 (http://www.arb-silva.de/).

Metagenomic 16S rRNA gene sequence reconstruction
16S rRNA gene fragments from Illumina metagenomic sequencing (described below) were reconstructed into near full-length genes using EMIRGE (Miller *et al.*, 2011) with 120 iterations and the non-redundant SILVA SSURef102 as the starting database. In the final iteration, 12 032 paired reads (0.05%) were reconstructed into 16S rRNA gene sequences. Sequences were clustered into OTUs⩾97% similar. To exclude less reliable rare sequences, OTUs with raw relative abundances ⩾0.5% were used. Representative sequences were BLASTed to the SILVA database. OTU abundances, calculated on the basis of a probabilistic accounting of read depth, were normalized by sequence lengths.

Phylogenetic analyses
For 16S rRNA phylogenetic analysis genes were aligned to reference sequences from GenBank with Clustal W (Thompson *et al.*, 1994), and Maximum Likelihood trees were created (see Handley *et al.*, 2012). Bootstrap consensus trees were inferred from 1000 replicates. Branches corresponding to partitions reproduced in <50% bootstrap replicates were collapsed. Trees were annotated with data sets in iTOL (Letunic and Bork, 2006).

Metagenome sequencing and assembly
Genomic DNA from the acetate-amended sediment was sequenced on one flow-cell of an Illumina Genome Analyzer IIx (Illumina, Inc., San Diego, CA, USA). A paired-end (PE) shotgun library with 1-kb insert size was prepared using Illumina's Genomic DNA Sample Prep kit, according to the manufacturer's instructions. Sequencing produced ~7 Gb of sequence (*versus* ~400 Mb with 454), and 29 million paired-end reads ~125-bp long. See Supplementary Information for further details, and a description of 454 sequencing and assembly. Illumina reads were trimmed to remove low-quality bases from the 3′ ends, after which 87% of paired/single reads >60-bp long were retained. Reads were initially assembled eight times using Velvet 1.1 (Zerbino and Birney, 2008) with different parameters optimized on the basis of expected genome coverage, after which a reference-guided Velvet-Columbus re-assembly was undertaken using paired-end scaffolds from the most abundant organism (r9c1, see binning section below and Supplementary Information for details).

Genome annotation
Genes were predicted, and translated into protein sequences using Prodigal (Hyatt *et al.*, 2010), and annotated using the pipeline, as described by Yelton *et al.* (2011).

Genomic binning of metagenomic assemblies
Emergent self-organizing maps of tetranucleotide frequencies and read coverage data were used to define bins (Dick *et al.*, 2009). Sequence fragments 5-kb long were used to create the map and separate sequences into bins, after which 2-kb fragments were projected onto the map. Emergent self-organizing maps (ESOM) were created using Databionic ESOM Tools (Ultsch and Mörchen, 2005). PE-scaffolds >2-kb long were also evaluated on the basis of read coverage (that is, relative abundance), gene GC-content and BLASTP best matches to the Uniref90 database (Suzek *et al.*, 2007) to help resolve unclear ESOM bin boundaries and classify low-abundance organisms. EMIRGE-reconstructed 16S rRNA sequences were assigned to genomic bins on the basis of the nearest BLAST-determined database match, read coverage and sequence abundance.

Genome completeness
Genome completeness was determined on the basis of 35 single-copy orthologous groups (OGs) (Raes *et al.*, 2007). OGs were obtained from eggNOG v. 3.0, a database of OGs in 1133 taxonomically diverse organisms, including 943 Bacteria (Powell *et al.*, 2012). Sequences were considered orthologous on the basis of reciprocal BLASTP analysis, if they had a minimum bit score of 60, an alignment length of ⩾70%, and ⩾30% shared identity.

Whole-genome comparisons
Relationships of assembled genomes to closely related genomes were measured using the amino-acid percent identity averaged across putative

orthologs, determined using reciprocal BLASTP with the same criteria as for genome completeness estimates.

Proteomics

Proteins were extracted from ~10 g of un-amended and acetate-amended sediment *via* a heat-assisted SDS-based method, followed by TCA protein precipitation/acetone washes, trypsin proteolysis, desalting and solvent exchange (Chourey *et al.*, 2010). Digested peptides were loaded in triplicate onto 5 cm strong cation-exchange columns, and connected to a reverse-phase (C18) front column (Phenomenex, Torrance, CA, USA) with an integrated nanospray tip (New Objective, Inc., Woburn, MA, USA). Proteomes were analyzed *via* two-dimensional 24-hour separations with CH_3COONH_4 salt pulses followed by reverse-phase gradients (Dionex U3000 HPLC, Sunnyvale, CA, USA) with online electrospray tandem mass spectrometry (2D-LC-MS/MS, LTQ Velos Orbitrap, Thermo Scientific, San Jose, CA, USA). Data-dependent MS/MS spectra were acquired, with full scans (400–1700 m/z) at 30-K resolution (top-ten method; dynamic exclusion: one; see VerBerkmoes *et al.*, 2009). MS/MS spectra were queried with SEQUEST (Eng *et al.*, 1994), against a predicted protein database constructed from the Velvet-Columbus metagenome assembly, along with common contaminants. Identified peptide sequences were reassembled into proteins and filtered with DTASelect (Tabb *et al.*, 2002) using the following parameters: Xcorr values >1.8 $(+1)$, 2.5 $(+2)$ and 3.5 $(+3)$ and DeltCN values >0.08, and a requirement for $\geqslant 2$ peptides per locus. The DTASelect and metagenomic database files are available at https://compbio.ornl.gov/ersp_rifle/column_sediment_2009. Summed triplicate technical replicates and normalized spectral abundance factors (NSAFs, Florens *et al.*, 2006) were used for subsequent analyses.

Modeling

The Supplementary Information describes a combined thermodynamic–kinetic modeling approach for microbially mediated rate laws on the basis of work of Jin and Bethke (2005) and Dale *et al* (2008).

Simulations of microbially mediated biogeochemical reactions (see below) were on the basis of physical and acetate-delivery parameters for well P104 and site geochemical data (Figure 1). The system was treated as one dimensional, with average flow and acetate delivery rates estimated from the arrival time of the bromide tracer (3.37 cm per day). Nitrate is present in micromolar concentrations within the aquifer near well P104 (Williams *et al.*, 2011), and varies 2 orders of magnitude across the site (unpublished data). For modeling, we used upper and lower values of 72 μM and 5 μM nitrate, with the latter value being more representative of the aquifer local to P104.

The rate of denitrification is affected by the maximum rate per unit cell or mass of biomass, v_{max}, and the biomass concentration, B_{mass}. Lacking cell-count information for the sulfur-oxidizing bacteria, we assumed a rate constant that implicitly accounts for the biomass and results in substantial denitrification over the 0.5-m flow path. We assumed the autotrophic (sulfide-dependent) denitrification reaction rate to be five times slower than heterotrophic denitrification, following Koenig and Liu (2001 and references therein) and Cardoso *et al.*

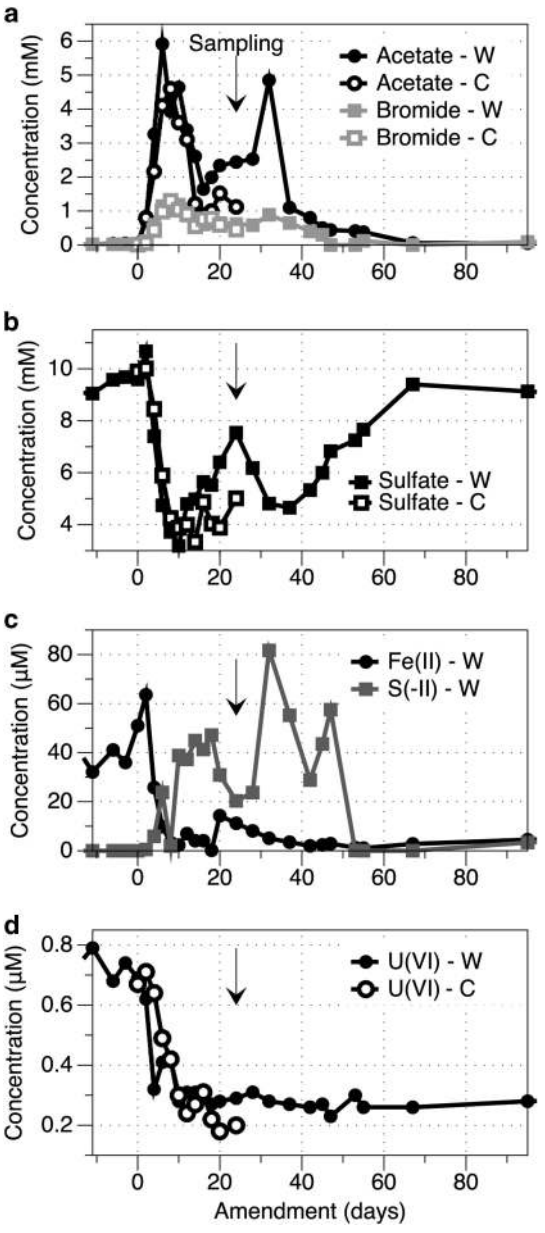

Figure 1 Plot showing concentrations of (**a**) acetate and bromide, (**b**) sulfate, (**c**) Fe(II) and sulfide, and (**d**) U(VI) in the column effluent (C, open symbols) and well bore (W, closed symbols) throughout the experiment. The column represents an extension of the amended aquifer, and no clear difference between C and W values is evident.

(2006) who showed S^0-dependent autotrophic denitrification is 10 times slower than heterotrophic denitrification, and the rate of denitrification with sulfide is twice as fast as with S^0. Comparisons were also made using an equal rate for autotrophic and heterotrophic pathways.

A half-saturation constant (that is, substrate concentration, where the specific growth rate equals half its maximum rate) of 2.1 μM NO_3^- (0.03 mg l^{-1} NO_3^--N, determined for the reaction $S^0 \rightarrow$ sulfate; Batchelor and Lawrence, 1978) was used for the autotrophic denitrification pathway. This is close to a value, 3 μM, determined by Claus and Kutzner (1985), and to the values reported for aerobic sulfide oxidation (Sorokin *et al.*, 2003). A range of half-saturation constants, 11.4 –142 μM NO_3^- (0.16–2 mg l^{-1} NO_3^--N), were used for the heterotrophic pathway-based values from the literature determined with either sludge or methanol as an organic carbon source (Engberg and Schroeder, 1975; Æsøy and Ødegaard, 1994; Henze *et al.* 2000; Klas *et al.*, 2006; Sarioglu *et al.*, 2009).

The catabolic reactions considered in the modeling are:

$$0.125SO_4^{2-} + 0.125CH_3COO^- + 0.125H^+ \xrightarrow[\text{Sulfate Reduction}]{} 0.125H_2S_{(aq)} + 0.25CO_{2(aq)}$$

$$0.5H_2S_{(aq)} + 0.2H^+ + 0.2NO_3^- \xrightarrow[\substack{\text{Autotrophic Denitrification}\\ \text{Sulfide to Sulfur}}]{} 0.5S^0 + 0.1N_{2(aq)}$$

$$0.125H_2S_{(aq)} + 0.05H^+ + 0.2NO_3^- \xrightarrow[\substack{\text{Autotrophic Denitrification}\\ \text{Sulfide to Sulfate}}]{} 0.125SO_4^{2-} + 0.1N_{2(aq)}$$

$$0.2NO_3^- + 0.125CH_3COO^- + 0.325H^+ \xrightarrow[\text{Heterotrophic Denitrification}]{} 0.1N_{2(aq)} + 0.25CO_{2(aq)}$$

with log equilibrium constants of 3.8305, 18.2813, 13.5785 and 19.1559, respectively.

Accession numbers

Reconstructed and cloned 16S rRNA gene sequences have been deposited in GenBank under the accession numbers JX125436–JX125454 and JX120370–JX120502, respectively. Metagenomic data are accessible through DDBJ/EMBL/GenBank (SRX149542 and AMQJ00000000 (version one: AMQJ01000000), BioProject PRJNA167727), and at http://banfieldlab.berkeley.edu/2009RifleSedimentMetagenome/.

Results and Discussion

Community composition and biogeochemical response to amendment

Previous studies have documented a period of Fe(III) reduction, followed by sulfate reduction in the Rifle aquifer during acetate amendment experiments, and concomitant reduction of U(VI) (Anderson *et al.*, 2003; Williams *et al.*, 2011). Periods marked by Fe(III) and sulfate reduction were accompanied by enrichments of *Desulfuromonadales,* and then *Peptococcaceae* followed by *Desulfobacterales* (Anderson *et al.*, 2003; Handley *et al.*, 2012). A legacy effect in the stimulated portions of the aquifer was observed to cause earlier onset of sulfate reduction upon subsequent re-stimulation, reducing the time from >1 month to <1 week over three subsequent experiments (Callister *et al.*, 2010; Williams *et al.*, 2011; Druhan *et al.*, 2012). In this study (a third-time stimulation experiment), the onset of sulfate reduction occurred within 2 days of acetate being detected in the incubation well (Figure 1a). Sediment was recovered after at least 18 days of sulfate reduction, during which time acetate remained in excess, and $U(VI)_{(aq)}$ and sulfate concentrations were halved (Figure 1b and d). Sulfide accumulation corresponded to the depletion of aqueous sulfate and Fe(II) (Figure 1c). The color of sediment throughout the column transformed from brown to black owing to the precipitation of FeS.

Clone and metagenome-derived (that is, EMIRGE-reconstructed) 16S rRNA gene data revealed a less even, lower diversity community after amendment (Figure 2a), consistent with earlier deeply-sampled 16S rRNA microarray analyses that measured ~40% lower OTU richness in the amended *versus* un-amended sediment (Handley *et al.*, 2012). Amendment enriched primarily for *Delta-* and *Epsilon-proteobacteria*, in particular a deltaproteobacterium closely related to the acetate-oxidizing SRB *Desulfobacter postgatei* (99% 16S rRNA gene sequence identity; Widdel and Pfennig, 1981). Other less-enriched bacteria are related to *Sulfurovum* and *Sulfurimonas*, *Geobacter* and *Desulfuromonas* and *Bacteroidetes* (Figure 2b). In general, three methods used for determining community composition and/or abundance (clone library, EMIRGE, read coverage) agreed (Supplementary Figures S2 and S3). The metagenome comprises a sample of highly abundant microorganisms; no archaeal 16S rRNA genes were detected.

Although previously un-amended sediment was used in the column, the community composition in both the column sediment, and in a split-phase sediment–quartz column incubated for the same period in well P104, differed substantially from compositions observed in first-time stimulation experiments after a similar period of amendment (Anderson *et al.*, 2003; Handley *et al.*, 2012). Less difference was observed between the column communities and those from second-time experiments, including post-amendment sediment collected from P104 in the previous year (Handley *et al.*, 2012). This tends to suggest the sediment (and quartz) were influenced by the local, twice previously stimulated, aquifer community.

Assembled genomes

After assembling Illumina reads (Table 1), we obtained genomes from seven different phylogenetic groups (Figure 3), and allocated 99% of sequence length >2-kb long to a genomic bin (Figure 4a). Phylogenetic analyses indicate that the binned

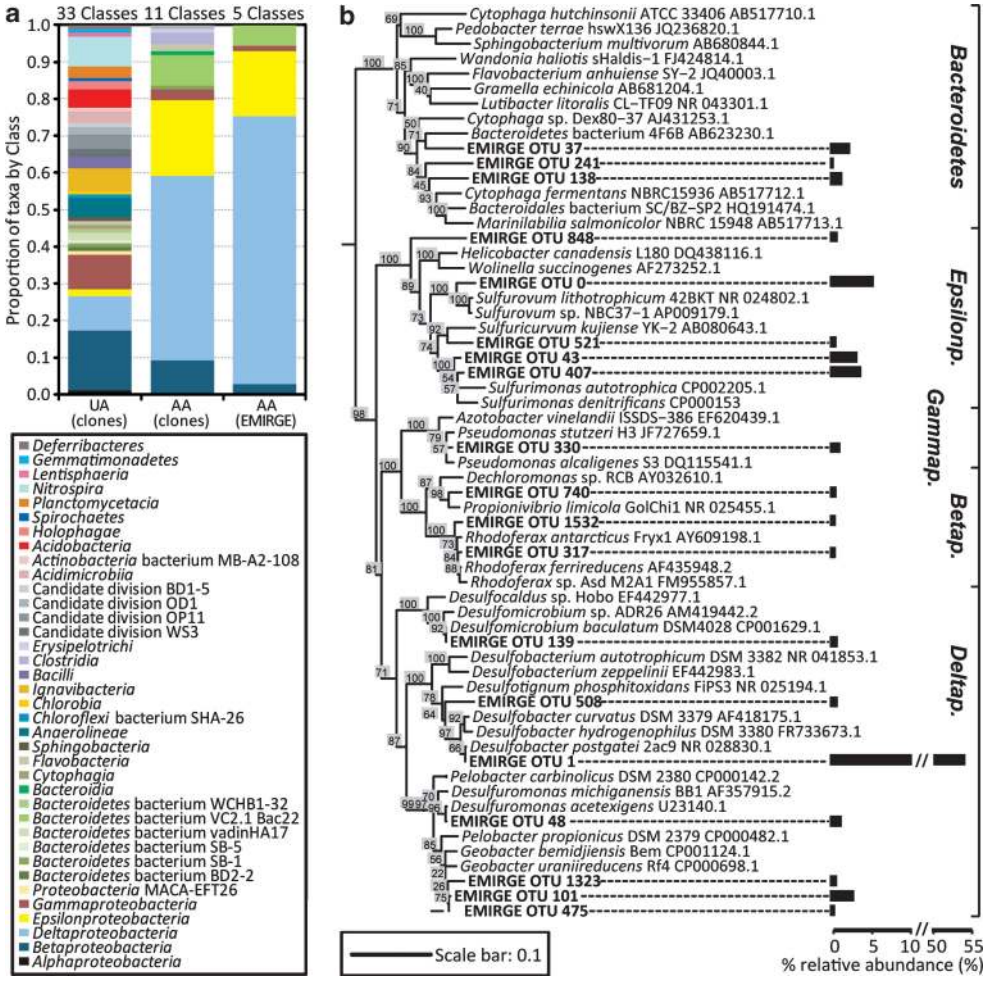

Figure 2 Community composition. (**a**) Relative abundances of Classes in the un-amended (UA) and acetate-amended (AA) communities determined using 16S rRNA gene clone libraries (UA and AA) or EMIRGE-reconstructed 16S rRNA genes from the metagenome (AA). (**b**) Bootstrap consensus tree of EMIRGE-reconstructed 16S rRNA gene sequences (AA). The tree is rooted to *Methanococcus vannielii* SB (CP000742.1). The scale bar (LHS) indicates the number of nucleotide substitutions per site. Bootstrap values are shown as percentages. A similar topology was obtained with the initial ML tree. Black bars indicate the OTU relative abundances in the metagenome. *Proteobacteria* classes are abbreviated.

genomes belong to: *Deltaproteobacteria* (r9c1, r9c7 -r9c8), *Epsilonproteobacteria* (r9c2-r9c3), *Bacteroidetes* (r9c4-r9c5) and *Firmicutes* (r9c6) (Table 2). All the genomes, except for the low-coverage *Firmicutes* genome, are represented by EMIRGE-reconstructed 16S rRNA sequences. Clone library data indicate the most abundant *Firmicutes* in the amended sediment were *Clostridiales* bacteria related to *Gracilibacteraceae* or *Peptococcaceae* (data not shown). However, greater similarity to a representative *Clostridiales* genome as opposed to *Peptococcaceae* is indicated by the average amino-acid identities of orthologs (Table 2).

We estimate that the seven major genomic bins comprise ~6 near-complete and three at least half-complete genomes (Figure 4b), of which, r9c1 and r9c2 each contain a single near-complete genome, with the latter being in two PE-scaffolds (1.9 and 0.1-Mb long). R9c3 and r9c5 each contain at least two near-complete genomes. The r9c7 bin contains partial-genome fragments closely related to *Geobacter* and *Desulfuromonas*. Similarity between these bacteria in terms of phylogeny, GC-content and abundance levels makes it difficult to resolve r9c7 genomes into separate bins.

Ortholog identities of >85% have been shown to correlate with DNA–DNA hybridization values of >70%, indicative of species level assignment (Goris *et al.*, 2007). On the basis of very high (96%) ortholog average amino-acid identity shared between r9c1 and *D. postgatei,* we suggest that they belong to same species. Excluding the small collection of r9c8 genes, which are very closely related to *Desulfomicrobium baculatum*, the other genomes have identities too low to sequenced genomes to suggest species assignment (Table 2).

Proteogenomics

A total of 1695 proteins and 112 606 peptides (93% unique peptides) from the acetate-amended samples were identified by liquid chromatography–

Table 1 Summary statistics for the Illumina Velvet and Velvet-Columbus assemblies, and the 454 Newbler assembly

Parameters	*Illumina + Velvet*[a]	*Illumina + Columbus*[a]	*Newbler + 454*[b]
PE-scaffolds/contigs (# >500 bp)	11 622	10 499	17 963
N50 (kb, >500 bp)	7.7	35.2	1.8
Summed length (Mb)	48	58	27
Average length (kb)	3.8	5.6	1.5
Longest PE-scaffold/contig (kb)	114	1910	90

Abbreviation: PE, paired-end.
[a]Illumina contigs are scaffolded using paired-end information into supercontigs (PE-scaffolds), and contain Ns.
[b]454 contigs were ordered (but not joined) into 2046 scaffolds using mate-pair reads.

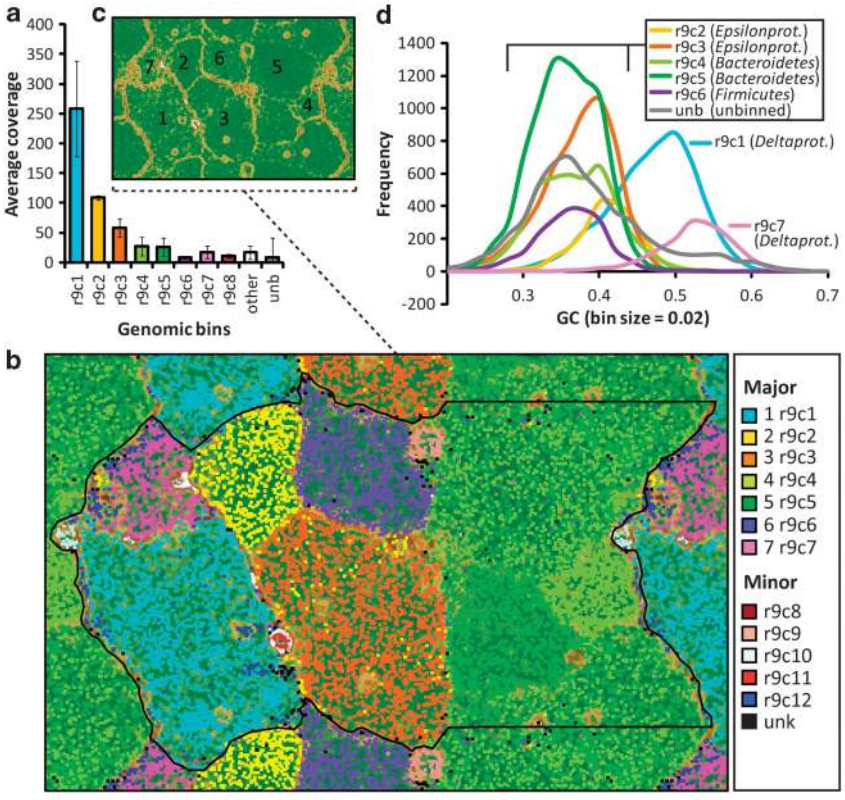

Figure 3 Genomic bins from the Illumina assembled data distinguished by (**a**) average read coverage per PE-scaffold ('other' includes bins r9c8-r9c12 and unk; 'unb' comprises unassigned fragments 500–2000 bp long), (**b**, **c**) ESOM (repeating tiled view—the black line demarks one representation of each genomic bin), and (**d**) GC content per gene. In the ESOM, several major genomic bins occur as distinct clusters demarked by topographic highs (beige lines, **c**). Two minor fragmentary genomic bins (r9c8 and r9c12) were not substantial or distinct enough from clusters 1 and 7 to form separate clusters in the ESOM, but both group with the *Deltaproteobacteria*. The three small ESOM clusters, r9c9–r9c11, are putative plasmid sequences, characterized by genes associated with transmembrane regions, DNA polymerase, phage, coiled-coil proteins, and a large number of hypothetical genes. 'Unk' are phylogenetically unassigned fragments >2 kb long. (**c**) ESOM without data points. Dark green denotes areas of high similarity. *Epsilonprot, Epsilonproteobacteria*; *Deltaprot., Deltaproteobacteria*.

tandem mass spectrometry using the metagenome as a protein reference database (Supplementary Dataset). Little digestible protein was present, and few (~31) proteins were identified in the unamended sediment after searching peptides against the same database (Supplementary Information), and are not discussed further.

Examination of organism-resolved proteins enabled detection of six bacterial groups (r9c1-r9c5 and r9c7) active during the amendment experiment (Figure 5; Supplementary Information/Data set). All groups expressed proteins associated with acetate utilization or carbon fixation *via* the TCA cycle. Among other key enzymes detected were those used in ribosomes, cell division, glycolysis/gluconeogenesis, acetate/acetyl-CoA formation, electron transport, nitrogen fixation, denitrification, sulfur respiration, phage resistance, chemotaxis and motility and response to oxidative stress. The majority of proteins detected (75% of proteins) and protein expression levels (95% of peptide spectral counts) are attributable to the dominant r9c1 genome.

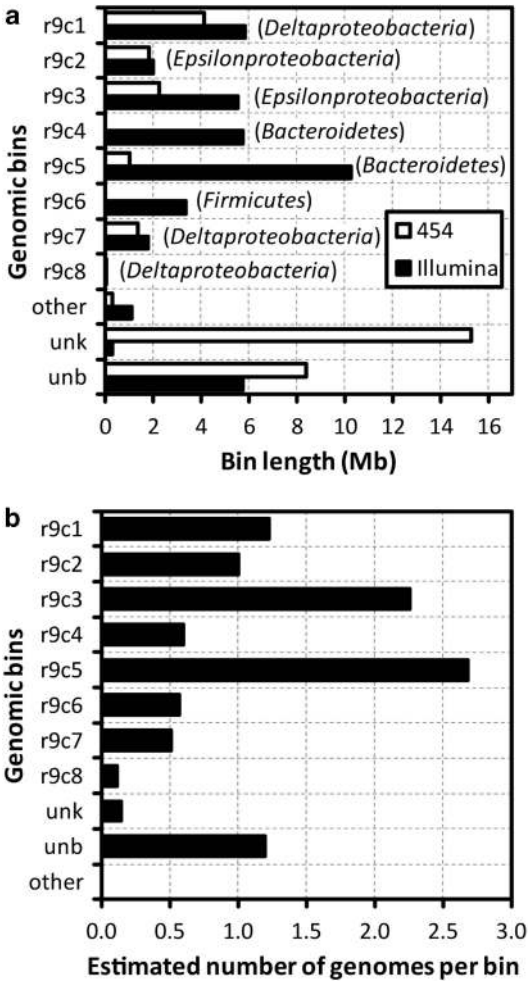

Figure 4 Plots showing (**a**) the length of sequence in Illumina- and 454-based genome bins; and (**b**) the estimated number of genomes per bin based on BLASTP searches for conserved OGs (bin lengths divided by estimated genome lengths). The sum of OGs detected in each bin was divided by the number of OGs queried (i.e. 35 *via* BLAST). 'Other' comprises bins r9c9-r9c12. 'Unb' comprises unassigned fragments 500–2000 bp long that contain predicted genes ('unk' are unassigned fragments >2 kb). Comparisons largely agree between estimates based on OGs and those determined based on the genome size of closely related organisms ($R^2 = 0.86$; Supplementary Figure S4) even though genome sizes of related organisms can only be considered as an approximate guide.

Activity and genomic potential of enriched bacteria

Acetate-oxidizing SRB. Amending the system with acetate created a niche ecosystem for *Desulfobacter* (r9c1), which proteomic data indicate actively respired sulfate coupled to acetate oxidation (Figures 5a–c). *Desulfobacter* species (almost) dedicatedly couple anaerobic acetate oxidation to the reduction of sulfate, and were originally considered marine bacteria, before the isolation of a freshwater sediment strain (Widdel and Pfennig, 1981; Widdel, 1987). Within the Rifle aquifer, acetate-stimulated enrichments of *Desulfobacteraceae* appear to supersede enrichments of sulfate-reducing *Peptococcaceae* (Anderson *et al.*, 2003; Handley *et al.*, 2012), although the reason for this is currently undetermined.

In this study, key proteins essential for the activation and reduction of sulfate were only detected for r9c1 (Figures 5 and 6a), including proteins potentially involved in the transfer of electrons from the membrane to APS and sulfite (QmoABC and HmeCDE; Mander *et al.*, 2002; Pires *et al.*, 2003; Mussman *et al.*, 2005). Genes were identified for *sat1* and *hmeB*, but were not represented in the proteome. In addition, almost all proteins necessary for gluconeogenesis were detected (Supplementary Information/Data set). Proteomic data (Figure 5) further indicate that r9c1 was actively dividing; chemotactic; motile by means of flagella and twitching pili; uptaking ammonium; and fixing nitrogen, possibly assisted by Rnf in electron transport (Schmehl *et al.*, 1993). Nitrogenase and ammonium transporter *amtB* have been shown to be co-expressed by acetate-stimulated blooms of *Geobacteraceae* in the Rifle aquifer during peak Fe(III) reduction (Mouser *et al.*, 2009). Expression of *amtB* transporter (and sensor) increases as ammonium concentrations approach zero (Javelle *et al.*, 2004; Mouser *et al.*, 2009) and nitrogen fixation becomes feasible (Helber *et al.*, 1988; Holmes *et al.*, 2004). While the high relative abundance of r9c1 was probably supported by nitrogen fixation, this seems unlikely to have conferred a substantial competitive advantage to r9c1 over other resident SRB (Handley *et al.*, 2012)—many of which are associated with genera containing diazotrophs (Zehr *et al.*, 2003).

We detected all but one r9c1 protein needed to oxidize acetate using a modified TCA cycle (Table 3). This cycle is used by *Desulfobacter* species instead of the acetyl-CoA pathway, which is used by other acetate-oxidizing SRB (Thauer *et al.*, 1989). The modified cycle makes use of 2-oxoglutarate:ferredoxin oxidoreductase and a reversible citrate lyase, which generate reduced ferredoxin instead of NADH and an extra ATP, respectively (Brandis-Heep *et al.*, 1983; Müller *et al.*, 1987; Müller-Zinkhan and Thauer, 1988). Neither the expected membrane-bound malate:quinone oxidoreductase (EC:1.1.5.4; Brandis-Heep *et al.*, 1983) nor the typical TCA cycle malate dehydrogenase (NADH-forming) was identified in the r9c1 genome by homology searches. While this could be an artifact of genome incompleteness, divergent homology or an unidentified analog, proteomics identified a pyruvate-forming malate dehydrogenase (NAD^+/$NADP^+$), which may potentially bypass this step, and regenerate oxaloacetate *via* pyruvate carboxylase or phosphoenolpyruvate (PEP) (cf. Hansen and Juni, 1979). Proteins for succinyl-CoA synthetase and for acetate activation by acetate kinase and phosphate acetyltransferase were identified by proteomics; however, identification of acetyl-CoA transferase suggests that r9c1 also used CoA transferase/hydrolase for both acetate activation and

Table 2 Summary data of genomic bins on the final Illumina Velvet–Columbus assembly

Bin	*Longest PE-scaffold (kb)*	*PE-scaffold (#)*	*ARC*[a] *(s.d.)*	*ORFs (#)*	*Proteins (#)*	*Related organisms*	*AAIO*[b] *(s.d.)*	*16S ID*[c]
Deltaproteobacteria								
r9c1	250	161	258 (80)	5421	1282	*Desulfobacter postgatei*	96 (7) F	99*
						Desulfobacterium autotrophicum	60 (14) D	89†
r9c7	60	294	17 (11)	1390	23	*Geobacter bemidjiensis*	66 (18) F	98*1
						Desulfuromonas michiganensis	–	97*2
						Desulfuromonas acetoxidans	59 (17) D	–
r9c8	20	11	11 (4)	41	0	*Desulfomicrobium baculatum*	88 (20) F	99*
Epsilonproteobacteria								
r9c2	1 910	2	109 (3)	1998	67	*Sulfurovum* sp. NBC37-1	71 (14) F	95*
r9c3	690	138	58 (15)	5678	160	*Sulfurimonas denitrificans*	79 (13) F	96*
						Sulfurimonas autotrophica	69 (15) F	94†
Bacteroidetes[d]								
r9c4	530	498	27 (15)	3936	52	*Cytophaga hutchinsonii*	50 (12) F	83†
r9c5	370	840	26 (16)	7321	78	*Cytophaga hutchinsonii*	50 (12) F	83†
						Wandonia haliotis	–	88*1
						Cytophaga fermentans	–	90*2
Firmicutes								
r9c6	60	395	8 (2)	1873	2	*Clostridium cellulovorans*	76 (25) F	–
						Desulfosporosinus orientis	52 (13) F	–
Other								
r9c9-r9c12	20–40	2–162	17 (11)	17–512	0–6	–	–	–

Abbreviations: ARC, average read coverage; AAIO, average amino acid identity of orthologs; D, draft reference genome; F, fully-curated reference genome; 16S ID, percent identity between 16S rRNA genes; ORFs, predicted genes; #, number.
[a]ARC was calculated from k-mer coverage.
[b]Using less strict criteria for determining orthologs (i.e., without a bit-score cutoff of $\geqslant 60$) made $\leqslant 2\%$ difference to calculated AAIs for most of the genome bins (r9c1–r9c5), but decreased AAIs by 3–6% for r9c6 and r9c8, and by 14% for r9c7.
[c]Percent identity match between EMIRGE-reconstructed and GenBank 16S rRNA sequences.
[d]The determined AAI of orthologs between r9c4 and r9c5 is 53%.
* denotes the nearest isolate sequence—*1 and *2 indicate where two reconstructed 16S rRNA gene sequences correlate to a single bin (r9c7), or cannot be assigned to one of the two bins (r9c4 and r9c5). † denotes matches to other organisms for comparison.

succinate formation (Figure 6b), as has been demonstrated for *D. postgatei*, *Desulfuromonas acetoxidans* and *Geobacter* species (Brandis-Heep *et al.*, 1983; Gebhardt *et al.*, 1985; Wilkins *et al.*, 2009).

In contrast to r9c1, *Desulfomicrobium* (r9c8) was less enriched. Members of this sulfate-reducing genus are incomplete oxidizers and are only known to use acetate mixotrophically with H_2 (Dias *et al.*, 2008). Assuming that r9c8 was also reducing sulfate, or other inorganic compounds respired by *Desulfomicrobium* species (for example, thiosulfate and nitrate), then it would likely have been substrate limited, and dependent on the production of H_2 or organic acids by other community members. Most *Desulfomicrobium* species are also able to ferment select organic acids (Dias *et al.*, 2008).

Other acetate oxidizers. Few proteins were identified from *Desulfuromonadales* r9c7, owing partly to incomplete genomes (Table 2, Figure 4b). Proteins and genes identified may be attributed to either the *Geobacter*- or *Desulfuromonas*-like bacteria comprising the r9c7 bin. Some genes, but no proteins, were detected for nitrogen fixation, ATP synthase, cell division, gluconeogenesis and motility by pili or flagella, and only one protein was detected for chemotaxis. Several key TCA cycle proteins were detected (Figures 5a and d; Table 3), demonstrating that *Desulfuromonadales* were actively consuming acetate, while sulfate reduction prevailed as the major terminal electron-accepting process. These bacteria do not reduce sulfate, but are well-known for their ability to reduce metals (including iron and uranium) and other inorganic elements or compounds (Lovley *et al.*, 2004).

Studies have demonstrated a correlation between the addition of simple organic substrates, such as glucose and organic acids like acetate, to terrestrial aquifers and the enrichment of Fe(III)-reducing *Geobacter* species (Snoeyenbos-West *et al.*, 2000; Holmes *et al.*, 2002, 2007). Repeat experiments amending the Rifle aquifer with acetate have consistently produced blooms of *Geobacter* associated with Fe(III) and U(VI) reduction (for example,

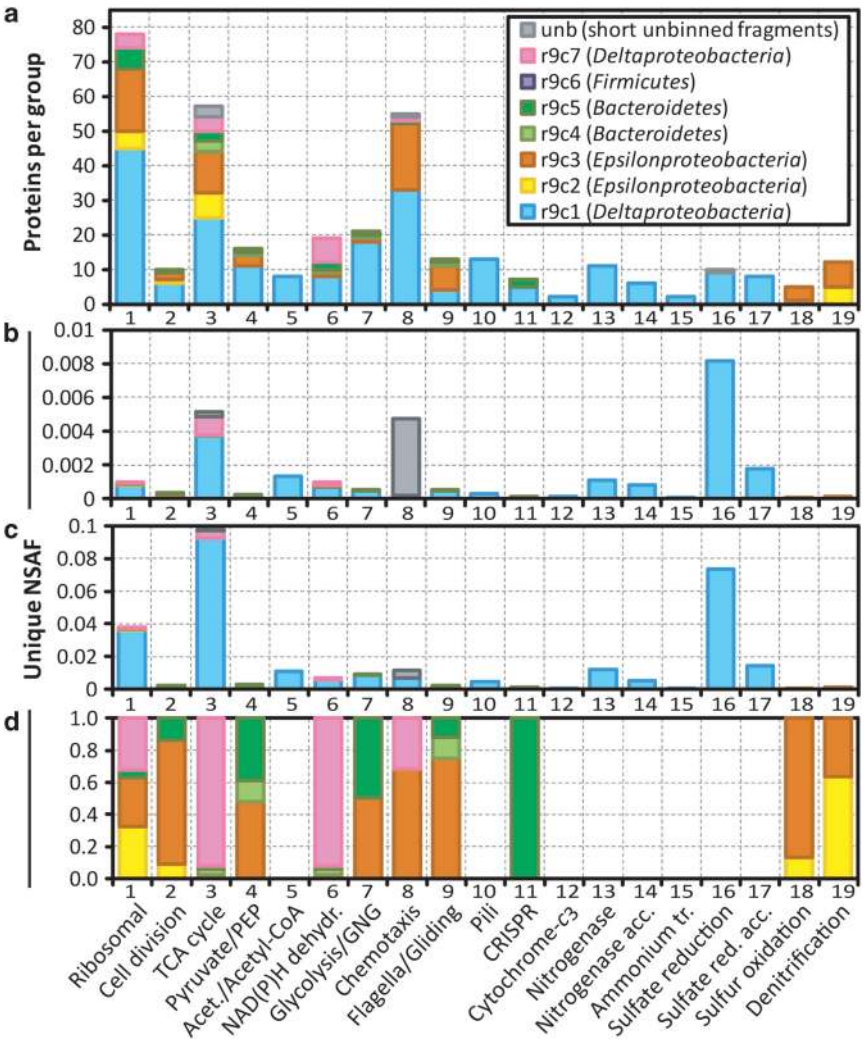

Figure 5 Proteins expressed in key functional groups (Supplementary Dataset) are shown as (**a**) number of proteins identified per group, (**b**) averaged or (**c**) summed unique NSAFs, and (**d**) relative proportions of summed unique NSAFs with r9c1 and unb removed. Little difference was evident between non-unique (not shown) and unique NSAF charts, except the overall contribution of TCA cycle peptides was 0.5% less in the latter. No proteins within these groups were matched to the r9c6 *Firmicutes* genome. Abbreviations and definitions: (3) oxidative/reductive TCA cycle proteins (4) conversion between pyruvate and phosphoenolpyruvate (PEP); (5) conversion between acetate and acetyl-CoA; (6) NADH/NADPH dehydrogenase; (7) glycolysis/gluconeogenesis; (11) Cas proteins associated with Clustered Regularly Interspaced Short Palindromic Repeats, CRISPR; (12) cytochrome-c_3 and cytochrome-c_3 hydrogenase; (13) nitrogenase (NifABDEHKU); (14) putative nitrogenase accessory proteins RnfCDEG; (15) ammonium transport AmtB; (16) sulfate reduction proteins ATP-sulfurylase (Sat2), adenylyl sulfate (APS) reductase (AprAB), dissimilary sulfite reductase (DsrABCEFH); (17) putative accessory proteins heterodisulfide reductase-like menaquinol-oxidizing enzyme (HmeCDE) and quinone-interacting membrane-bound oxidoreductase (QmoABC); (18) sulfur oxidation proteins SoxCY and SQR; (19) NO_3^- (NapAB), NO_2 (NirS), NO (NorC), N_2O (NosZ) reductases (further details in Supplementary Text and Dataset).

Anderson *et al.*, 2003; Holmes *et al.*, 2007; Wilkins *et al.*, 2009). These enriched *Geobacter* and co-enriched *Desulfuromonas* species persist as significant community members, although at lower relative abundances, after sulfate reduction becomes prevalent (Handley *et al.*, 2012), and *Geobacter* are key candidates for the ongoing reductive immobilization of U(VI) observed during sulfate reduction in this study (Figure 1d). Despite the capacity for abiotic reduction of sulfide, microbial Fe(III) reduction may proceed concurrent with sulfate reduction (Sörensen, 1982; Tugel *et al.*, 1986; Canfield, 1989). It is therefore plausible that either genera attributed to the *Desulfuromonadales* r9c7 may have also coupled acetate-oxidation with Fe(III) reduction. Alternatively, r9c7 bacteria may have gained energy from S^0 reduction (Pfennig and Biebl, 1976; Lovley *et al.*, 2004), which has been shown to accumulate during acetate amendment of the Rifle aquifer. Williams *et al.* (2011) identified 4–5 mmol kg^{-1} S^0 (below 3-m depth) in the core collected to create well P104 (used in this study) after 110 days of acetate amendment (second year amendment). Comparably, little S^0 was identified in

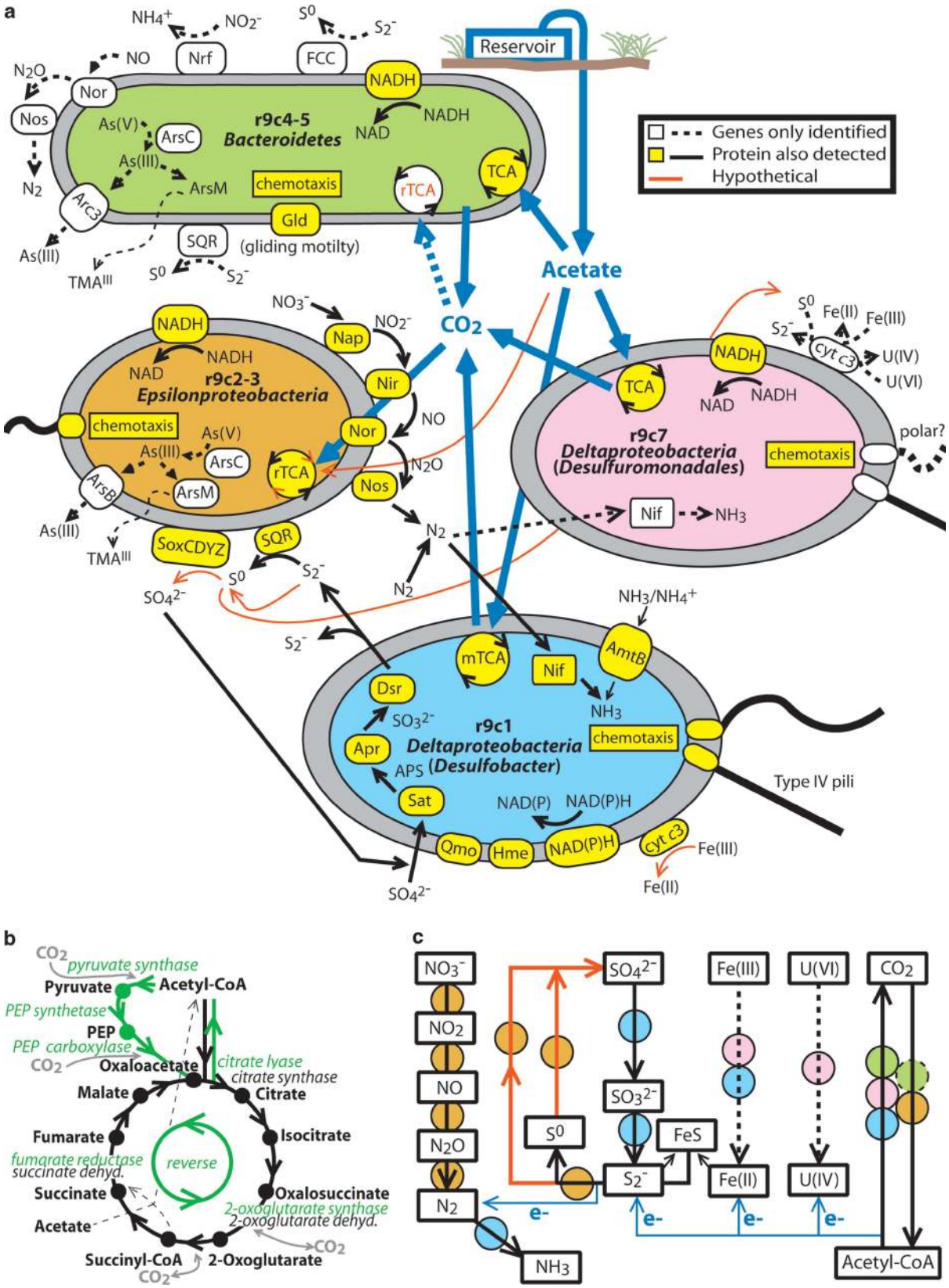

Figure 6 (**a**) Schematic of biogeochemical cycling and physiology inferred from genetic (white boxes) and proteomic (yellow boxes) data. (**b**) TCA cycle with enzymes necessary for the reductive cycle shown in green. The dashed line indicates the path with acetyl-CoA transferase (forming succinate and acetyl-CoA). (**c**) Summary biogeochemical redox reactions inferred from proteogenomic data. Colored circles correspond to the organisms in (**a**). rTCA, reductive TCA cycle; mTCA, modified TCA cycle; TMA^{III}, trimethylarsine gas; dehyd, dehydrogenase.

Table 3 TCA cycle and related components identified for genomic bins r9c1-5 and r9c7

#	*Enzyme*	*EC*	*1*	*2*	*3*	*4*	*5*	*7*
1	Citrate synthase	2.3.3.1	—	—	G	—	P	P
1	ATP citrate lyase	2.3.3.8	P	P	P	—	—	—
1	Citrate lyase	4.1.3.6	P	G	G	G	G	—
2	Aconitate hydratase	4.2.1.3	P	G	P	—	G	G
3	Isocitrate dehydrogenase	1.1.1.41/42	P	P	P	P	G	—
4a	2-oxoglutarate dehydrogenase E1	1.2.4.2	—	—	—	G	—	—
4b	2-oxoglutarate dehydrogenase E2	2.3.1.61	—	—	—	G	G	—
4c	Dihydrolipoamide dehydrogenase	1.8.1.4	P	—	—	G	G	—
4	2-oxoglutarate synthase	1.2.7.3	P	P	P	G	G	—
5	Succinyl-CoA synthetase	6.2.1.4/5	P	P	P	G	G	—
6	Succinate/fumarate reductase	1.3.5.1[a]	P	P	—	P	P	P
7	Fumarate hydratase	4.2.1.2	P	G	G	—	G	—
8	Malate dehydrogenase (NAD-dependent)	1.1.1.37	—	P	G	P	G	P
8	Malate dehydrogenase (quinone)	1.1.5.4	—	—	G	G	—	—
	Related: pyruvate/PEP							
	PEP synthetase	2.7.9.2	P	G	G	G	G	—
	PEP carboxylase (GTP)	4.1.1.32	P	—	—	—	—	—
	PEP carboxylase (ATP)	4.1.1.49	—	—	—	—	—	—
	PEP carboxylase	4.1.1.31	G	—	—	—	P	—
	Pyruvate/oxaloacetate carboxylase	6.4.1.1[b]	P	P	P	G	G	—
	Pyruvate ferredoxin oxidoreductase	1.2.7.1	P	G	P	P	—	—
a	Pyruvate dehydrogenase E1	1.2.4.1	P	G	—	G	G	—
b	Pyruvate dehydrogenase E2	2.3.1.12	P	—	—	—	—	—
c	(4c above)							
	Related: acetate↔acetyl-CoA							
	Acetyl-CoA hydrolase/transferase	3.1.2.1	P	—	—	—	G	—
	Acetyl-CoA synthetase	6.2.1.1	P	G	G	—	—	—
a	Acetate kinase (acetyl-P↔acetate)	2.7.2.1	P	G	G	G	G	—
a	Acylphophatase (acetyl-P→acetate)	3.6.1.7		G	—	G	G	—
b	Phosphate acetyltransferase	2.3.1.8	P	G	G	G	G	—

Abbeviations: #, order of TCA cycle reactions in the oxidative direction; EC, enzyme commission number; G, genes only identified; P, proteins also detected.
Reactions for enzymes not previously defined here: pyruvate carboxylase (pyruvate→oxaloacetate); pyruvate ferredoxin oxidoreductase (i.e., pyruvate synthase; pyruvate↔acetyl-CoA); pyruvate dehydrogenase and dihydrolipoamide dehydrogenase (pyruvate↔acetyl-CoA).
[a]Succinate/fumarate reductase equates to EC:1.3.5.1/EC:1.3.99.1.
[b]pyruvate carboxylase equates to EC:6.4.1.1/EC:4.1.1.3.

less-stimulated sediment cores collected further from the acetate source.

Bacteroidetes, on the other hand, are well-known for their ability to degrade carbohydrates and other complex organic compounds using respiratory or fermentative metabolisms (Holmes *et al.*, 2007; Lee *et al.*, 2010; Thomas *et al.*, 2011). A number of genes identified here are associated with mannose metabolism (mannose-1-phosphate guanyltransferase, mannose-6-phosphate isomerase, GDP-mannose 4,6-dehydratase, phosphomannomutase), xylan degradation (candidate β-xylosidase, endo-1,4-β-xylanase) and cellulose degradation (family 3 candidate β-glycosidase), including identification of *Bacteroidetes*-like unbinned partial fragments (0.5–2 kb long) resembling candidate β-glycosidase and cellobiose phosphorylase. However, few expressed proteins indicative of these metabolisms were identified. Only two proteins (with peptide counts just above detection) were identified that are suggestive of cellobiose degradation and mannose metabolism (candidate β-glycosidase hydrolase, phosphomannomutase), and only two glycolysis proteins were detected.

Instead, detection of some key TCA cycle enzymes, including citrate synthase (Figures 5a and d; Table 3), suggests that the *Bacteroidetes* may have been using the cycle heterotrophically to oxidize acetate (cf. Xie *et al.*, 2007; Zhang *et al.*, 2009), although use of the reductive cycle cannot be excluded. Genomic data indicate that *Bacteroidetes* r9c5 has a complete oxidative TCA cycle (near-complete in r9c4), and both r9c4 and r9c5 have genes that may support a reductive cycle (that is, citrate lyase, 2-oxoglutarate synthase, pyruvate synthase, PEP synthetase and carboxylase). The electron acceptor for this reaction is not evident; however, on the basis of genomic evidence, one possibility is that *Bacteroidetes* coupled acetate oxidation to the reduction of nitrogen species, as genes were identified for nitric-oxide reductase (*norABD*) and nitrous-oxide reductase (*nosLZ*).

Genes were also identified for a formate-dependent, ammonium-forming nitrite(/polysulfide) reductase (*nrfADH*); selenate reductase *ygfK* (r9c4 only); sulfur metabolism, namely SQR (r9c4 only), a *Chlorobium luteolum*-like flavocytochrome-*c* sulfide dehydrogenase and a *phsC*-like

cytochrome-b_{561} thiosulfate reductase; and arsenic detoxification (similar to r9c2-r9c3; Figure 6a). Although the experimental condition under which *Bacteroidetes* r9c4 and r9c5 were growing was anoxic, genes for cytochrome-*c* and cytochrome-*bd* oxidase and cytochrome-cbb_3 oxidase (*ccoPQNOS*) indicate a capacity for these bacteria to also grow (micro)aerobically (Preisig *et al.*, 1993; Trumpower and Gennis, 1994; Visser *et al.*, 1997; Kulajta *et al.*, 2006).

Sulfur oxidizers: acetate-induced syntrophy. Previously, researchers have demonstrated syntrophic growth between oxygen-dependent, sulfide-oxidizing *Thiobacillus thioparus* and sulfate-/S^0-reducing, *Desulfovibrio desulfuricans* in co-culture, such that a positive-feedback cycle was established between the reductive and oxidative processes of these two bacteria (van den Ende *et al.*, 1997). In another study, geochemical and functional gene-based evidence for a cryptic microbial sulfur cycle, suggests that this process may have important biogeochemical consequences for sulfate recycling in oceanic oxygen minimum zones (Canfield *et al.*, 2010). Proteogenomic results here indicate that a similar process was operating in the acetate-amended Rifle aquifer sediment, and suggest that syntrophic growth of autotrophic or possibly mixotrophic *Sulfurovum*- and *Sulfurimonas*-like bacteria (r9c2 and r9c3) were supported by sulfide and CO_2 generated by heterotrophic respiration.

Species within these two epsilonproteobacterial genera are autotrophic, and oxidize sulfide, sulfur and thiosulfate either with oxygen and/or nitrate serving as electron acceptors (Hoor, 1975; Inagaki *et al.*, 2003, 2004). *Sulfurimonas denitrificans* oxidizes sulfide by reducing nitrate completely to N_2 (Hoor, 1975). According to genomic studies of *Sulfurovum* sp. NBC37-1 and *S. denitrificans* DSM1251, sulfur oxidation in these organisms may proceed *via* the sulfur oxidation pathway (SoxCDYZXAB), forming sulfate, or SQR, forming S^0 from sulfide (Nakagawa *et al.*, 2007; Sievert *et al.*, 2008).

Similarly, r9c2 and r9c3 possess respiratory genes for a complete denitrification pathway (*napABDFGHL*, *nirSF, nirNJ* for r9c3 only, *norBC*, *nosZ*), sulfur oxidation (SQR, *soxCDYZ*) excluding *soxXAB* (Supplementary Figure S5), and also the reductive TCA cycle for CO_2 fixation (Table 3; Figure 6b). Proteomic data infer that, during amendment these *Epsilonproteobacteria* performed nitrate-dependent sulfide/sulfur oxidation coupled to CO_2 fixation *via* the reductive TCA cycle (Figures 5a and d). However, simultaneous operation of an oxidative TCA cycle to support mixotrophic growth with acetate cannot be excluded (cf. Tang and Blankenship, 2010). Proteomics further show r9c2 and r9c3 were dividing, and r9c3 was chemotactic and motile. Genes for cytochrome-cbb_3 oxidase (*ccoPQONS*), cytochrome-b_{561} (r9c3; Murakami *et al.*, 1986) and cytochrome-*bd* (r9c2) suggest that these bacteria could also oxidize sulfur (micro)aerobically.

The missing *soxXAB* genes (not detected by homology searches) are normally required for thiosulfate (and presumably sulfide and sulfur) attachment to SoxYZ, activation to sulfane, and release after oxidation by SoxCD (Friedrich *et al.*, 2005; Sauvé *et al.*, 2007; Zander *et al.*, 2011). Hence, the exact function of Sox in sulfur oxidation by r9c2 and r9c3 cannot be deduced from our data. Green sulfur bacteria lacking *soxCD* (but with functional *soxXAB* and *soxYZ* genes) are able to use *dsr* with or without *apr* genes in reverse to oxidize sulfide or sulfite, respectively (Sakurai *et al.*, 2010; Gregersen *et al.*, 2011). We identified no genes indicative of a reverse sulfate reduction pathway in r9c2 and r9c3. Nevertheless, *in vitro* enzyme assays by Rother *et al.* (2001) suggest sulfide or S^0 oxidation may proceed, although at a slower rate (13–19 or 3–17 times less, respectively), without either SoxXA or SoxB. The same is true for SoxXAB without SoxCD or SoxYZ.

Synteny is shared between *soxXAB* and *soxCDYZ* in the model organism, *Paracoccus pantotrophus*, and several other *Alphaproteobacteria* (Friedrich *et al.*, 2005). However, they form two non-syntenous gene clusters in bacteria closely related to r9c2 and r9c3, *Sulfurovum* sp. NBC37-1 and *S. denitrificans* DSM1251 (Nakagawa *et al.*, 2007; Sievert *et al.*, 2008; Supplementary Figure S5). In as much as conservation of gene order tends to suggest conservation of gene function, loss of synteny tends to suggest a loss of co-dependence between the gene clusters, possibly occurring with increased evolutionary distance (Yelton *et al.*, 2011). This may explain the apparent loss of *soxXAB* genes in r9c2 and r9c3.

While it is possible that r9c2 and r9c3 completely re-oxidized sulfide to sulfate, an autotrophic denitrifying community from anaerobic sludge has been shown to only partially oxidize sulfide (probably to S^0) when placed under nitrate-limiting conditions, but completely oxidize sulfide to sulfate with unlimited nitrate (Cardoso *et al.*, 2006). Considering the micromolar concentrations of nitrate available in the aquifer (Williams *et al.*, 2011), this could also reasonably explain the enrichment of bacteria in this study (r9c2 and r9c3) that are potentially only able to oxidize sulfide to S^0. Any formation of S^0 by these bacteria would likely be re-cycled by putative sulfur-reducing bacteria, r9c7.

Autotrophic versus heterotrophic denitrification

Simulations of biogeochemical processes occurring during acetate amendment captured the general features of the acetate and sulfate breakthrough curves at well P104, and estimate nitrate conversion to N_2 (Supplementary Figures S6a and b). Although simulations for autotrophic (sulfide-dependent) and heterotrophic (acetate-dependent) denitrification

use estimates for nitrate and specific growth rates, and exclude biomass, analyses indicate that the autotrophic denitrification pathway, involving sulfide oxidation to S^0 or sulfate, is thermodynamically feasible. Despite its greater standard Gibbs energy of reaction, the autotrophic sulfide to sulfate pathway is less favored than the sulfide to S^0 pathway (Supplementary Figure S6c) because of the high sulfate concentration in groundwater (Figure 1b).

Although heterotrophic denitrification is thermodynamically favored over autotrophic denitrification (ΔG of ca. -220 *versus* -178 kJ per electron per mole), the effect is insignificant if the thermodynamic factor (F_T) formulation in Equation 3 (Supplementary Information; Supplementary Figure S6c) is assumed to be correct, as the system is effectively far from equilibrium with respect to both pathways, and F_T is very close to 1. This implies that behavior is controlled by the Monod kinetic terms in Equation 2 (Supplementary Information). Principally owing to the low half-saturation constant used for autotrophic denitrification, simulations for the sulfide–sulfur reaction tend to indicate that the autotrophic pathway dominates over the heterotrophic pathway given a concentration of 5 μM (at all considered heterotrophic versus autotrophic rates), and vice versa for the higher 72-μM concentration when assuming a slower autotrophic rate (Supplementary Figure S6d–i). While a potential impact of sulfide toxicity on community composition and function cannot be excluded, modeling results may explain why, with acetate in excess, autotrophic sulfide-dependent denitrification by *Epsilonproteobacteria* r9c2 and r9c3 out-competed heterotrophic denitrification in this experiment. Another factor may be possible mixotrophic growth by *Epsilonproteobacteria* r9c2 or r9c3, which would likely increase cell growth and denitrification rates (Cardoso *et al*., 2006).

Conclusions

We reconstructed the genomes of members of a subsurface sediment community enriched during acetate amendment. Proteomics identified organism-specific function and syntrophic interactions among community members (Figures 6a and c). While the dominant process identified was acetate-fueled sulfate reduction, excess acetate was also respired by enriched *Desulfuromonadales*, probably supporting concurrent Fe(III)-, U(VI)- and/or S^0-reduction. Gene-based evidence and TCA cycle proteins detected for *Bacteroidetes* suggest that they contributed to acetate degradation, and have the capacity for reducing nitrogen species. Co-enrichment of *Epsilonproteobacteria* and expression of proteins associated with sulfide oxidation and carbon fixation imply that products of heterotrophic acetate oxidation—sulfide and CO_2—were used as a carbon and energy source by autotrophic or mixotrophic *Epsilonproteobacteria*. Sulfide-dependent denitrification may have been favored over the heterotrophic pathway owing to nitrate-limiting conditions within the Rifle aquifer, such that kinetic factors govern outcomes. In turn, reaction products of epsilonproteobacterial metabolism, such as N_2, were probably fixed and sulfate or S^0 respired by *Desulfobacter* or *Desulfuromonadales* bacteria. These results suggest acetate-amendment promoted complex organismal and metabolic processes and interactions involved in carbon, sulfur, metal and nitrogen cycling.

Acknowledgements

Funding was provided through the IFRC, Subsurface Biogeochemical Research Program, Office of Science, Biological and Environmental Research, the US Department of Energy (DOE), with equal support for LBNL employees through LBNL's Sustainable Systems Scientific Focus Area (contract DE-AC02-05CH11231); and an EMBO Long-Term Fellowship (I Sharon). Genomic sequencing was performed at the W M Keck Center for Comparative and Functional Genomics, University of Illinois at Urbana-Champaign. We thank S Chan (University of California, LA, USA) for help with field implementation, and K Campbell (the US Geological Survey, Menlo Park) and J Bargar (Stanford Synchrotron Radiation Lightsource, Menlo Park, USA) for assistance with column design. We also thank our anonymous reviewer's for their helpful comments.

References

Altschul SF, Gish W, Miller W, Myers EW, Lipman DJ. (1990). Basic local alignment search tool. *J Mol Biol* **215**: 403–410.

Anderson RT, Vrionis HA, Ortiz-Bernad I, Resch CT, Long PE, Dayvault R *et al.* (2003). Stimulating the *in situ* activity of *Geobacter* species to remove uranium from the groundwater of a uranium-contaminated aquifer. *Appl Environ Microbiol* **69**: 5884–5891.

Batchelor B, Lawrence AW. (1978). Autotrophic denitrification using elemental sulfur. *J Water Pollut Control Fed* **50**: 1986–2001.

Benner R, Maccubbin AE, Hodson RE. (1984). Anaerobic biodegradation of the lignin and polysaccharide components of lignocellulose and synthetic lignin by sediment microflora. *Appl Environ Microbiol* **47**: 998–1004.

Brandis-Heep A, Gebhardt NA, Thauer RK, Widdel F, Pfennig N. (1983). Anaerobic acetate oxidation to CO_2 by *Desulfobacter postgatei* 1. Demonstration of all enzymes required for the operation of the citric acid cycle. *Arch Microbiol* **136**: 222–229.

Callister SJ, Wilkins MJ, Nicora CD, Williams KH, Banfield JF, VerBerkmoes NC *et al.* (2010). Analysis of biostimulated microbial communities from two field experiments reveals temporal and spatial differences in proteome profiles. *Environ Sci Technol* **44**: 8897–8903.

Canfield DE. (1989). [Reactive iron in marine sediments]. *Geochimica et Cosmochimica Acta* **53**: 619–632.

Canfield DE, Stewart FJ, Thamdrup B, De Brabandere L, Dalsgaard T, Delong EF *et al.* (2010). A cryptic sulfur

cycle in oxygen-minimum-zone water off the Chilean Coast. *Science* **330**: 1375–1378.
Cardoso RB, Sierra-Alvarez R, Rowlette P, Flores ER, Gómez J, Field JA. (2006). Sulfide oxidation under chemolithoautotrophic denitrifying conditions. *Biotech Bioeng* **95**: 1148–1157.
Chourey K, Jansson J, VerBerkmoes N, Shah M, Chavarria KL, Tom LM *et al.* (2010). Direct cellular lysis/protein extraction protocol for soil metaproteomics. *J Proteome Res* **9**: 6615–6622.
Claus G, Kutzner HJ. (1985). Physiology and kinetics of autotrophic denitrification by *Thiobacillus denitrificans*. *Appl Microbiol Biotechnol* **22**: 283–288.
Dale AW, Regnier P, Knab NJ, Jørgensen BB, Van Cappellen P. (2008). [Anaerobic oxidation of methane (AOM) in marine sediments from Skagerrak (Denmark): II. Reaction-transport modeling]. *Geochimica et Cosmochimica Acta* **72**: 2880–2894.
Dias M, Salvado JC, Monperrus M, Caumette P, Amouroux D, Duran R *et al.* (2008). Characterization of Desulfomicrobium salsuginis sp. nov. and Desulfomicrobium aestuarii sp. nov., two new sulfate-reducing bacteria isolated from the Adour estuary (French Atlantic coast) with specific mercury methylation potentials. *Syst Appl Microbiol* **31**: 30–37.
Dick GJ, Andersson AF, Baker BJ, Simmons SL, Thomas BC, Yelton AP *et al.* (2009). Community-wide analysis of microbial genome sequence signatures. *Genome Biol* **10**: R85.
Druhan JL, Steefel CI, Molins S, Williams KH, Conrad ME, DePaolo DJ. (2012). Timing the onset of sulfate reduction over multiple subsurface acetate amendments by measurement and modeling of sulfur isotope fractionation. *Environ Sci Technol* **46**: 8895–8902.
Edgar RC. (2010). Search and clustering orders of magnitude faster than BLAST. *Bioinformatics* **26**: 2460–2461.
Eng JK, McCormack AL, Yates JR. (1994). An approach to correlate tandem mass spectral data of peptides with amino acid sequences in a protein database. *J Am Soc Mass Spectrom* **5**: 976–989.
Engberg DJ, Schroeder ED. (1975). Kinetics and stoichiometry of bacterial denitrification as a function of cell residence time. *Water Res* **9**: 1051–1054.
Florens L, Carozza MJ, Swanson SK, Fournier M, Coleman MK, Workman JL *et al.* (2006). Analyzing chromatin remodeling complexes using shotgun proteomics and normalized spectral abundance factors. *Methods* **40**: 303–311.
Friedrich CG, Bardischewsky F, Rother D, Quentmeier A, Fischer J. (2005). Prokaryotic sulfur oxidation. *Curr Opin Microbiol* **8**: 253–259.
Fuchs G. (1986). CO_2 fixation in acetogenic bacteria. *FEMS Microbiol Rev* **39**: 181–213.
Gebhardt NA, Thauer RK, Linder D, Kaulfers P-M, Pfennig N. (1985). Mechanism of acetate oxidation to CO_2 with elemental sulfur in Desulfuromonas acetoxidans. *Arch Microbiol* **141**: 392–398.
Gibson GR. (1990). Physiology and ecology of the sulphate-reducing bacteria. *J Appl Bacteriol* **69**: 769–797.
Goris J, Konstantinidis KT, Klappenbach JA, Coenye T, Vandamme P, Tiedje JM. (2007). DNA-DNA hybridization values and their relationship to whole-genome sequence similarities. *Int J Syst Evol Microbiol* **57**: 81–97.
Gregersen LH, Bryant DA, Frigaard N-U. (2011). Mechanisms and evolution of oxidative sulfur metabolism in green sulfur bacteria. *Front Microbiol* **2**: 116.
Handley KM, Wrighton KC, Piceno YM, Andersen GL, DeSantis TZ, Williams KH *et al.* (2012). High-density PhyloChip profiling of stimulated aquifer microbial communities reveals a complex response to acetate amendment. *FEMS Microbiol Ecol* **81**: 188–204.
Hansen EJ, Juni E. (1979). Properties of mutants of *Escherichia coli* lacking malic dehydrogenase and their revertants. *J Biol Chem* **254**: 3570–3575.
Hartog N, Van Bergen PF, De Leeuw JW, Griffioen J. (2004). [Reactivity of organic matter in aquifer sediments: geological and geochemical controls]. *Geochimica et Cosmochimica Acta* **68**: 1281–1292.
Hazen TC, Dubinsky EA, DeSantis TZ, Andersen GL, Piceno YM, Singh N *et al.* (2010). Deep-sea oil plume enriches indigenous oil-degrading bacteria. *Science* **330**: 204–208.
Helber JT, Johnson TR, Yarbrough LR, Hirschberg R. (1988). Effect of nitrogenous compounds on nitrogenase gene expression in anaerobic cultures of Anabaena variabilis. *J Bacteriol* **170**: 558–563.
Henze M, Gujer W, Mino T, van Loosdrecht M. (2000). *Activated Sludge Models ASM1, ASM2, AMS2(d) and ASM3. IWA Scientific and Technical Report Series*. IWA Publishing: London, UK.
Holmes DE, Finneran KT, O'Neil RA, Lovley DR. (2002). Enrichment of members of the family *Geobacteraceae* associated with stimulation of dissimilatory metal reduction in uranium-contaminated aquifer sediments. *Appl Environ Microbiol* **68**: 2300–2306.
Holmes DE, Nevin KP, Lovley DR. (2004). *In situ* expression of *nifD in Geobacteraceae* in subsurface sediments. *Appl Environ Microbiol* **70**: 7251–7259.
Holmes DE, Nevin KP, Woodard TL, Peacock AD, Lovley DR. (2007). *Prolixibacter bellariivorans* gen. nov., sp. nov., a sugar-fermenting, psychrotolerant anaerobe of the phylum *Bacteroidetes*, isolated from a marine-sediment fuel cell. *Int J Syst Evol Microbiol* **57**: 701–707.
Holmes DE, O'Neil RA, Chavan MA, N'Guessan LA, Perpetua LA, Larrahondo MJ *et al.* (2009). Transcriptome of *Geobacter uraniireducens* growing in uranium-contaminated subsurface sediments. *ISME J* **3**: 216–230.
Holmes DE, O'Neil RA, Vrionis HA, N'Guessan LA, Ortiz-Bernad I, Larrahondo MJ *et al.* (2007). Subsurface clade of *Geobacteraceae* that predominates in a diversity of Fe(III)-reducing subsurface environments. *ISME J* **1**: 663–677.
Hoor AT-T. (1975). A new type of thiosulphate oxidizing, nitrate reducing microorganism: *Thiomicrospira denitrificans* sp. nov. *Neth J Sea Res* **9**: 344–350.
Hyatt D, Chen GL, Locascio PF, Land ML, Larimer FW, Hauser LJ. (2010). Prodigal: prokaryotic gene recognition and translation initiation site identification. *BMC Bioinformatics* **11**: 119.
Inagaki F, Takai K, Kobayashi H, Nealson KH, Horikoshi K. (2003). *Sulfurimonas autotrophica* gen. nov., sp. nov., a novel sulfur-oxidizing -proteobacterium isolated from hydrothermal sediments in the Mid-Okinawa Trough. *Int J Syst Evol Microbiol* **53**: 1801–1805.
Inagaki F, Takai K, Kobayashi H, Nealson KH, Horikoshi K. (2004). *Sulfurovum lithotrophicum* gen. nov., sp. nov., a novel sulfur-oxidizing chemolithoautotroph within the -*Proteobacteria* isolated from Okinawa Trough hydrothermal sediments. *Int J Syst Evol Microbiol* **54**: 1477–1482.

Islam FS, Gault AG, Boothman C, Polya DA, Charnock JM, Chatterjee D *et al.* (2004). Role of metal-reducing bacteria in arsenic release from Bengal delta sediments. *Nature* **430**: 68–71.

Javelle A, Severi E, Thornton J, Merrick M. (2004). Ammonium sensing in Escherichia coli. role of the ammonium transporter AmtB and AmtB-GlnK complex formation. *J Biol Chem* **279**: 8530–8538.

Jin QA, Bethke CM. (2005). [Predicting the rate of microbial respiration in geochemical environments]. *Geochimica et Cosmochimica Acta* **69**: 1133–1143.

Karl DM, Church MJ, Dore JE, Letelier RM, Mahaffey C. (2012). Predictable and efficient carbon sequestration in the North Pacific Ocean supported by symbiotic nitrogen fixation. *Proc Natl Acad Sci* **109**: 1842–1849.

Klas S, Mozes N, Lahav O. (2006). Development of a single-sludge denitrification method for nitrate removal from RAS effluents: lab-scale results vs. model prediction. *Aquaculture* **259**: 342–353.

Koenig A, Liu LH. (2001). Kinetic model of autotrophic denitrification in sulphur packed-bed reactors. *Water Res* **35**: 1969–1978.

Kulajta C, Thumfart JO, Haid S, Daldal F, Koch H-G. (2006). Multi-step assembly pathway of the cbb_3-type cytochrome *c* oxidase complex. *J Mol biol* **355**: 989–1004.

Lane DJ. (1991). 16S/23S rRNA sequencing. In: Stackebrandt E, Goodfellow M (eds). *Nucleic Acid Techniques in Bacterial Systematics*. Wiley: New York, pp 115–148.

Lee D-H, Choi E-K, Moon S-R, Ahn S, Lee YS, Jung JS *et al.* (2010). *Wandonia haliotis* gen. nov., sp. nov., a marine bacterium of the family *Cryomorphaceae*, phylum. *Int J Syst Evol Microbiol* **60**: 510–514.

Leschine SB. (1995). Cellulose degradation in anaerobic environments. *Annu Rev Microbiol* **49**: 399–426.

Lovley DL, Holmes DE, Nevin KP. (2004). Dissimilatory Fe(III) and Mn(IV) reduction. *Adv Microb Physiol* **49**: 219–286.

Letunic I, Bork P. (2006). Interactive tree of life (iTOL): an online tool for phylogenetic tree display and annotation. *Bioinformatics* **23**: 127–128.

Mander GJ, Duin EC, Linder D, Stetter KO, Hedderich R. (2002). Purification and characterization of a membrane-bound enzyme complex from the sulfate-reducing archaeon *Archaeoglobus fulgidus* related to heterodisulfide reductase from methanogenic archaea. *Eur J Biochem* **269**: 1895–1904.

Miller CS, Baker BJ, Thomas BC, Singer SW, Banfield JF. (2011). EMIRGE: reconstruction of full-length ribosomal genes from microbial community short read sequencing data. *Genome Biol* **12**: R44 12.

Mouser PJ, N'Guessan AL, Elifantz H, Holmes DE, Williams KH, Wilkins MJ *et al.* (2009). Influence of heterogeneous ammonium availability on bacterial community structure and the expression of nitrogen fixation and ammonium transporter genes during *in situ* bioremediation of uranium-contaminated groundwater. *Environ Sci Technol* **43**: 4386–4392.

Murakami H, Kita K, Anraku Y. (1986). Purification and properties of a diheme cytochrome b_{561} of the *Escherichia coli* respiratory chain. *J Biol Chem* **261**: 548–551.

Mussman M, Richter M, Lombardot T, Meyerdierks A, Kuever J, Kube M *et al.* (2005). Clustered genes related to sulfate respiration in uncultured prokaryotes support the theory of their concomitant horizontal transfer. *J Bacteriol* **187**: 7126–7137.

Müller D, Schauder R, Fuchs G, Thauer RK. (1987). Acetate oxidation to CO_2 via a citric acid cycle involving an ATP-citrate lyase: a mechanism for the synthesis of ATP via substrate level phosphorylation in *Desulfobacter postgatei* growing on acetate and sulfate. *Arch Microbiol* **148**: 202–207.

Müller-Zinkhan D, Thauer RK. (1988). Membrane-bound NADPH dehydrogenase- and ferredoxin:NADP oxidoreductase activity involved in electron transport during acetate oxidation to CO_2 in *Desulfobacter postgatei*. *Arch Microbiol* **150**: 145–154.

Nakagawa S, Takaki Y, Shimamura S, Reysenbach A-L, Takai K, Horikoshi K. (2007). Deep-sea vent-proteobacterial genomes provide insights into emergence of pathogens. *Proc Natl Acad Sci USA* **104**: 12146–12150.

Pfennig N, Biebl H. (1976). *Desulfuromonas acetoxidans* gen. nov. and sp. nov., a new anaerobic, sulfur-reducing, acetate-oxidizing bacterium. *Arch Microbiol* **110**: 3–12.

Pires RH, Lourenço AI, Morais F, Teixeira M, Xavier AV, Saraiva LM *et al.* (2003). A novel membrane-bound respiratory complex from *Desulfovibrio desulfuricans* ATCC 27774. *Biochim Biophys Acta* **1605**: 67–82.

Powell S, Szklarczyk D, Trachana K, Roth A, Kuhn M, Muller J *et al.* (2012). eggnog v3.0: orthologous groups covering 1133 organisms at 41 different taxonomic ranges. *Nucleic Acids Res* **40**: D284–D289.

Preisig O, Anthamatten D, Hennecke H. (1993). Genes for a microaerobically induced oxidase complex in *Bradyrhizobium japonicum* are essential for a nitrogen-fixing endosymbiosis. *Proc Natl Acad Sci USA* **90**: 3309–3313.

Raes J, Korbel JO, Lercher MJ, von Mering C, Bork P. (2007). Prediction of effective genome size in metagenomic samples. *Genome Biol* **8**: R10.

Ram RJ, VerBerkmoes NC, Thelen MP, Tyson GW, Baker BJ, Blake RC II *et al.* (2005). Community proteomics of a natural microbial biofilm. *Science* **308**: 1915–1920.

Rother D, Henrich H-J, Quentmeier A, Bardischewsky F, Friedrich CG. (2001). Novel genes of the *sox* gene cluster, mutagenesis of the flavoprotein SoxF, and evidence for a general sulfur-oxidizing system in *Paracoccus pantotrophus* GB17. *J Bacteriol* **183**: 4499–4508.

Rowland HAL, Polya DA, Lloyd JR, Pancost RD. (2006). Characterisation of organic matter in a shallow, reducing, arsenic-rich aquifer, West Bengal. *Org Geochem* **37**: 1101–1114.

Sakurai H, Ogawa T, Shiga M, Inoue K. (2010). Inorganic sulfur oxidizing system in green sulfur bacteria. *Photosynth Res* **104**: 163–176.

Sarioglu M, Insel G, Arlan N, Orhon D. (2009). Model evaluation of simultaneous nitrification and denitrification in a membrane bioreactor operated without an anoxic reactor. *J Membr Sci* **337**: 17–27.

Sauvé V, Bruno S, Berks BC, Hemmings AM. (2007). The SoxYZ complex carries sulfur cycle intermediates on a peptide swinging arm. *J Biol Chem* **282**: 23194–23204.

Schmehl M, Jahn A, zu Vilsendorf AM, Hennecke S, Masephol B, Schuppler M. (1993). Identification of a new class of nitrogen fixation genes in *Rhodobacter capsulatus*: a putative membrane complex involved in electron transport to nitrogenase. *Mol Gen Genet* **241**: 602–615.

Sievert SM, Scott KM, Klotz MG, Chain PSG, Hauser LJ, Hemp J *et al.* (2008). Genome of the

epsilonproteobacterial chemolithoautotroph. *Sulfurimonas denitrificans* **74**: 1145–1156.

Snoeyenbos-West OL, Nevin KP, Anderson RT, Lovley DR. (2000). Enrichment of *Geobacter* species in response to stimulation of Fe(III) reduction in sandy aquifer sediments. *Microb Ecol* **39**: 153–167.

Sorokin DY, Banciu H, van Loosdrecht M, Kuenen JG. (2003). Growth physiology and competitive interaction of obligately chemolithoautotrophic, haloalkaliphilic, sulfur-oxidizing bacteria from soda lakes. *Extremophiles* **7**: 195–203.

Suzek BE, Huang H, McGarvey P, Mazumder R, Wu CH. (2007). UniRef: comprehensive and non-redundant UniProt reference clusters. *Bioinformatics* **23**: 1282–1288.

Sörensen J. (1982). Reduction of ferric iron in anaerobic, marine sediment and interaction with reduction of nitrate and sulfate. *Appl Environ Microbiol* **43**: 319–324.

Tabb DL, McDonald WH, Yates JR III. (2002). DTASelect and contrast: tools for assembling and comparing protein identifications from shotgun proteomics. *J Proteome Res* **1**: 21–26.

Tang KH, Blankenship RE. (2010). Both forward and reverse TCA cycles operate in green sulfur bacteria. *J Biol Chem* **285**: 35848–35854.

Thauer RK, Möller-Zinkhan D, Spormann AM. (1989). Biochemistry of acetate catabolism in anaerobic chemotrophic bacteria. *Annu Rev Microbiol* **43**: 43–67.

Thomas F, Hehemann J-H, Rebuffet E, Czjzek M, Michel G. (2011). Environmental and gut *Bacteroidetes*: the food connection. *Front Microbiol* **2**: 93.

Thompson JD, Higgins DG, Gibson TJ. (1994). CLUSTAL W: improving the sensitivity of progressive multiple sequence alignment through sequence weighting, position-specific gap penalties and weight matrix choice. *Nucleic Acids Res* **22**: 4673–4680.

Trumpower BL, Gennis RB. (1994). Energy transduction by cytochrome complexes in mitochondrial and bacterial respiration: the enzymology of coupling electron transfer reactions to transmembrane proton translocation. *Annu Rev Biochem* **63**: 675–716.

Tugel JB, Hines ME, Jones GE. (1986). Microbial iron reduction by enrichment cultures isolated from estuarine sediments. *Appl Environ Microbiol* **52**: 1167–1172.

Ultsch A, Mörchen F. (2005). *ESOM-Maps: tools for clustering, visualization, and classification with Emergent SOM.*. Department of Mathematics and Computer Science, University of Marburg: Germany, *Technical Report no. 46*.

van den Ende FP, Meier J, van Gemerden H. (1997). Syntrophic growth of sulfate-reducing bacteria and colorless sulfur bacteria during oxygen limitation. *FEMS Microbiol Ecol* **23**: 65–80.

VerBerkmoes NC, Russell AL, Shah M, Godzik A, Rosenquist M, Halfvarson J. (2009). Shotgun metaproteomics of the human distal gut microbiota. *ISME J* **3**: 179–189.

Visser JM, de Jong GAH, de Vries S, Robertson LA, Kuenen JG. (1997). cbb_3 cytochrome oxidase in the obligately chemolithoautotrophic *Thiobacillus* sp. W5. *FEMS Microbiol Lett* **147**: 127–132.

Whitman WB, Coleman DC, Wiebe WJ. (1998). Prokaryotes: the unseen majority. *Proc Natl Acad Sci USA* **95**: 6578–6583.

Widdel F. (1987). New types of acetate-oxidizing, sulfate-reducing *Desulfobacter* species, *D. hydrogenophilus* sp. nov., *D. latus* sp. nov., and *D. curvatus* sp. nov. *Arch Microbiol* **148**: 286–291.

Widdel F, Pfennig N. (1981). Studies on dissimilatory sulfate-reducing bacteria that decompose fatty acids I. isolation of new sulfate-reducing bacteria enriched with acetate from saline environments. Description of *Desulfobacter postgatei* gen. nov., sp. nov. *Arch Microbiol* **129**: 395–400.

Widdel F, Rabus R. (2001). Anaerobic biodegradation of saturated and aromatic hydrocarbons. *Curr Opin Biotechnol* **12**: 259–276.

Wilkins MJ, VerBerkmoes NC, Williams KH, Callister SJ, Mouser PJ, Elifantz H *et al.* (2009). Proteogenomic monitoring of *Geobacter* physiology during stimulated uranium bioremediation. *Appl Environ Microbiol* **75**: 6591–6599.

Williams KH, Long PE, Davis JA, Wilkins MJ, N'Guessan AL, Steefel CI *et al.* (2011). Acetate availability and its influence on sustainable bioremediation of uranium-contaminated groundwater. *Geomicro J* **28**: 519–539.

Xie G, Bruce DC, Challacombe JF, Chertkov O, Detter JC, Gilna P *et al.* (2007). Genome sequence of the cellulolytic gliding bacterium *Cytophaga hutchinsonii*. *Appl Environ Microbiol* **73**: 3536–3546.

Yelton AP, Thomas BC, Simmons SL, Wilmes P, Zemla A, Thelen MP *et al.* (2011). A semi-quantitiative, synteny-based method to improve functional predictions for hypothetical and poorly annotated bacterial and archaeal genes. *PLoS Comput Biol* **7**: e1002230.

Zander U, Faust A, Klink BU, de Sanctis D, Panjikar S, Quentmeier A *et al.* (2011). Structural basis for the oxidation of protein-bound sulfur by the sulfur cycle molybdohemo-enzyme sulfane dehydrogenase SoxCD. *J Biol Chem* **286**: 8349–8360.

Zehr JP, Jenkins BD, Short SM, Steward GF. (2003). Nitrogenase gene diversity and microbial community structure: a cross-system comparison. *Environ Microbiol* **5**: 539–554.

Zerbino DR, Birney E. (2008). Velvet: algorithms for *de novo* short read assembly using de Bruijn graphs. *Genome Res* **18**: 821–829.

Zhang L, Dai J, Tang Y, Luo X, Wang Y, An H *et al.* (2009). *Hymenobacter deserti* sp. nov., isolated from the desert of Xinjiang, China. *Int J Syst Evol Microbiol* **59**: 77–82.

Æsøy A, Ødegaard H. (1994). Denitrification in biofilms with biologically hydrolysed sludge as carbon source. *Wat Sci* **29**: 93–100.

Supplementary Information accompanies the paper on The ISME Journal website (http://www.nature.com/ismej)